Materials Science & Engineering A 667 (2016) 147–155

Contents lists available at ScienceDirect

Materials Science & Engineering A

journal homepage: www.elsevier.com/locate/msea

Precipitation kinetics during aging of an alumina-forming austenitic stainless steel

Geneva Trotter [a], Bin Hu [a], Annie Y. Sun [a], Reed Harder [a], M.K. Miller [b], Lan Yao [b], Ian Baker [a,*]

[a] Thayer School of Engineering, Dartmouth College, Hanover, NH 03755, USA
[b] Center for Nanophase Materials Sciences, Oak Ridge National Laboratory, Oak Ridge, TN 37831, USA

ARTICLE INFO

Article history:
Received 15 February 2016
Received in revised form
25 April 2016
Accepted 26 April 2016
Available online 28 April 2016

Keywords:
Austenite
Intermetallics
Aging
Coarsening
Grain boundaries
Precipitation

ABSTRACT

The microstructural evolution of DAFA26, an alumina-forming austenitic (AFA) stainless steel, was investigated during aging. The effect of aging at 750 °C and 800 °C on the growth of spherical γ'-Ni_3(Al, Ti) particles present in the as-processed state was studied extensively using X-ray diffraction, microhardness testing, scanning electron microscopy, transmission electron microscopy, and atom probe tomography. The γ' particles had a cube-on-cube orientation relationship with the matrix (i.e. ($(010)_m//(010)_p$, $[100]_m//[100]_p$)). The coarsening kinetics of γ'-Ni_3Al particles were in agreement with the Lifshitz, Slyozof-Wagner theory. Coarse Laves phase particles were also present in the as-processed state, and during the aging process both smaller Laves phase precipitates and B2-NiAl precipitates formed on both the grain boundaries and in the matrix. The γ' precipitates were determined to have the most impact on the room temperature hardness.

1. Introduction

Currently there is an effort to develop new materials that will enable fossil fuel-burning power plants to operate more efficiently. In order to work in power plants that can operate in the ultra super critical (USC) range of 760 °C/35 MPa, the materials used for these systems must have excellent creep and corrosion resistance. Efficiency improvements as well as reduced CO_2 emissions are benefits that can be realized with the higher operating temperatures obtained with advanced materials [1–4]. Alloyed with aluminum to provide corrosion resistance, alumina-forming austenitic (AFA) stainless steels have shown promise for application in the harsh environments seen in energy production where strong materials that are both oxidation and corrosion resistant are needed [5–16].

AFAs have a wide composition range and continued study of this system is needed to find the optimal combination of alloying elements that provide the best creep strength while maintaining good oxidation and corrosion resistance at minimal cost for future commercialization [16]. The B2-NiAl phase is commonly found in AFAs at temperatures below 900 °C due to the Al and Ni additions needed for alumina-scale formation and promotion of a single-phase matrix [15]. Nb is added because it increases oxidation resistance by improving the stability of the alumina-scale. The amount of Nb needed for this beneficial effect promotes Fe_2Nb phase formation [6,8,13,15]. In the newer grades of AFAs, the austenitic matrix needed for creep strength can be obtained, and MC-base precipitates or γ'-Ni_3Al have been added for creep strength [9,14,16]. Optimization of these alloys is difficult because the effects that different alloying elements and precipitates have on the creep strength of these steels are complex and oftentimes not well understood.

Recently, there has been a shift in focus on the development of AFAs. AFAs have traditionally been strengthened by MC and/or $M_{23}C_6$ carbides [16], and creep resistance in an AFA was shown to improve with an increase in nanoscale MC precipitates [11,14]. Earlier studies of AFAs have noted the presence of γ' precipitates [16,17], and new studies of AFAs have shown that nano-scale γ'–Ni_3(Al, Ti) precipitates can be used to improve creep resistance [15]. The present study utilizes X-ray diffraction (XRD), scanning electron microscopy (SEM), transmission electron microscopy (TEM), and atom probe tomography (APT) to investigate the microstructural evolution of precipitates during aging in an Fe-14Cr-32Ni-3Nb-0.15Si-(3 – 4)Al-(1 – 3)Ti-(0–0.3)Zr wt%. This alloy was named '32Z', where the '32Z' refers to 3Al-2Ti with Zr additions, and exhibited a longer creep-life than Fe-based Superalloy A286

* Correspondence to: 14 Engineering Drive, Dartmouth College, Hanover, NH 03755, USA
E-mail address: Ian.Baker@dartmouth.edu (I. Baker).

http://dx.doi.org/10.1016/j.msea.2016.04.081
0921-5093/

Table 1
AFA26 alloy composition (nominal and analyzed).

AFA26 (at%)	Fe	Cr	Ni	Al	Si	Nb	Ti	W	Zr	C	B	P	S	O	N
Nominal	44.7	14.8	29.9	6.1	0.3	1.8	2.3	–	0.2	–	–	–	–	–	–
Analyzed	44.56	14.79	30.39	5.97	0.25	1.74	2.26	0.003	0.006	0.009	< 0.002	< 0.004	< 0.0002	< 0.0041	< 0.0016

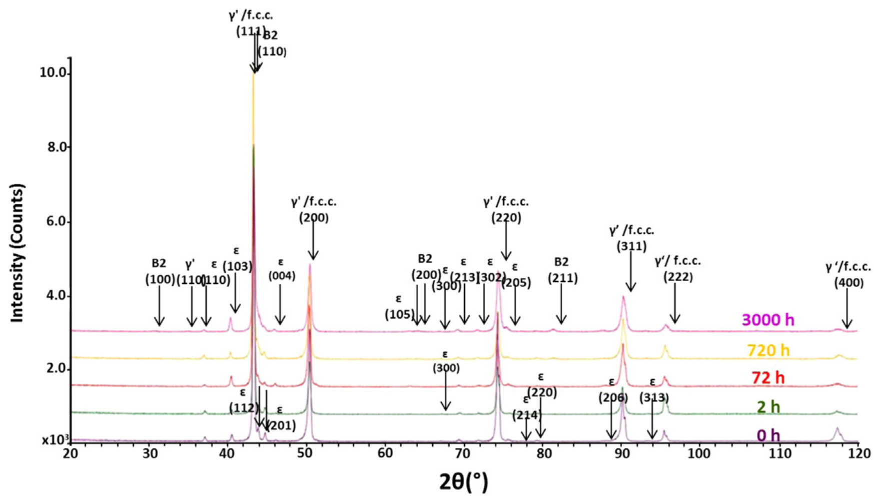

Fig. 1. XRD patterns of bulk AFA26 specimens with visible peaks labeled 'γ'' for the $L1_2$ particles, 'B2' for NiAl, and 'ε' for the Laves phase in the as-cast state and after aging at 2, 72, 720, and 3000 h.

when tested at 750 °C/100 MPa [15]. This paper calls the alloy 'AFA26,' which is similar to the title designated by Yamamoto et al. in [18]. AFA26 with the additions of C or B has been studied previously by Hu et al. and is referred to as 'AFA29' [19].

2. Experimental

The AFA26 specimens were processed at Oak Ridge National Laboratory (ORNL). 600 g ingots were arc-melted using pure element feedstock. The arc-melted ingots were then drop cast into a 1″ × 1″ × 3″ bar shaped die, soaked for 2 h at 1100 °C in Ar+4% H_2 gas, and then hot-rolled along the longitudinal axis with an approximately 15–20% thickness reduction per pass until the desired thickness reduction (up to 80%) was achieved. The same homogenization temperature of 1100 °C was then used to solutionize the plate for 30 min in Ar+4% H_2 gas, followed by air-cooling. Table 1 includes both the nominal composition and analyzed composition of AFA26.

XRD analysis of the AFA26 was performed using a Rigaku D/Max 2000 diffractometer using Cu Kα radiation (λ=0.1541 nm). Specimens were cut from treated ingots and polished with successively finer grits of silicon carbide paper up to 1200-grit, followed by polishing with 0.3 and 0.05 μm alumina powder in water to obtain a mirror finish. XRD measurements were performed by scanning 2θ from 20° to 140° using a step size of 0.02°. MDI Jade software was used to identify phases in the alloys and to analyze the diffraction patterns. A tube voltage of 40 kV and anode current of 300 mA was used.

Vickers microhardness data was used to provide insight into the alloy's aging characteristics. Specimens were mounted in phenolic resin and polished as described above to a mirror finish using 0.3 μm alumina powder. Tests were performed at room temperature using a TIME TH-713 Microhardness Tester under a load of 1.96 N (200 g) with a 15 s dwell time.

TEM, SEM, and APT analyses of the AFA26 were also performed. TEM specimens were prepared by cutting rectangular bars and milling them into 3 mm diameter cylinders. The cylinders were then cut into 3 mm discs, which were mechanically thinned and polished to ~150 μm thick and electropolished using a Struers TenuPol-5 twin-jet electropolisher at 11 V and ~180 mA in a solution of 25% nitric acid in methanol at −20 °C. The thin-foils were examined in an energy dispersive X-ray microanalysis (EDS)-equipped FEI Tecnai FS20ST field emission gun (FEG) TEM operated at 200 kV. The resulting thin foils were also examined in a FEI XL30 FEG SEM operated at 15 kV. APT analysis was performed at ORNL using a Cameca instruments local electrode atom probe (LEAP) 4000X HR. Specimens were annular milled in an FEI Nova 200 dual beam focused ion beam (FIB) equipped-SEM after being electropolished in a solution of 2% perchorlic acid and 98% 2-butoxyethanol. Some specimens were fabricated by FIB annular milling and a lift-out procedure [20]. During voltage-mode APT experiments, a specimen temperature of 50 K, a pulse fraction of 20%, and a pulse repetition rate of 200 kHz were used.

3. Results and discussion

The as-processed AFA26 had a grain size of 20 μm and showed a small amount of grain growth to 28 μm after aging for 3000 h. Fig. 1 shows XRD patterns of the AFA26 in the as-hot-rolled state and after aging for 2, 72, 720, and 3000 h at 750 °C. F.c.c., B2, γ', and Laves phase peaks are labeled. The f.c.c. and C14 Laves phase peaks are of similar intensities throughout the aging sequence, while the γ' and B2 peaks become more prominent as the aging time increases: the γ' (110) peak was only strong enough to be detected in the XRD pattern after the material had been aged for 3000 h. Lattice constant evaluation was done using the Pawley method [21] through the Whole Pattern Fitting routine in the MDI Jade software. The Pawley method is an approach that was designed to address problems caused by overlapping peaks and uses whole pattern fitting to extract integrated intensities and refine the peak positions. The lattice constant is calculated based on the γ' phase 2θ angles, including the lowest angle (110) peak. Whole pattern fitting of the diffraction pattern yielded lattice parameters for the specimens annealed for 3000 h. The lattice parameter of the f.c.c. matrix was calculated to be a=0.3602 nm and that for the γ' phase was a=0.3595 nm. Thus, the lattice misfit between the γ' precipitates and the f.c.c. matrix is −0.19%. The lattice parameter of the B2-NiAl was a=0.2892 nm and those for the C14 Fe_2Nb Laves phase, a=0.4823 nm and c=0.7865 nm.

AFA29 is an AFA stainless steel that has a similar nominal composition to the